



**University of  
Zurich**<sup>UZH</sup>

**Zurich Open Repository and  
Archive**

University of Zurich  
University Library  
Strickhofstrasse 39  
CH-8057 Zurich  
[www.zora.uzh.ch](http://www.zora.uzh.ch)

---

Year: 2016

---

**Long-distance dispersal after the last glacial maximum (LGM) led to the  
disjunctive distribution of *Pedicularis kansuensis* (Orobanchaceae) between  
the Qinghai-Tibetan plateau and Tianshan region**

Li, Wen-Jun ; Sui, Xiao-Lin ; Kuss, Patrick ; Liu, Yan-Yan ; Li, Ai-Rong ; Guan, Kai-Yun

DOI: <https://doi.org/10.1371/journal.pone.0165700>

Posted at the Zurich Open Repository and Archive, University of Zurich

ZORA URL: <https://doi.org/10.5167/uzh-127308>

Journal Article

Published Version

Originally published at:

Li, Wen-Jun; Sui, Xiao-Lin; Kuss, Patrick; Liu, Yan-Yan; Li, Ai-Rong; Guan, Kai-Yun (2016). Long-distance dispersal after the last glacial maximum (LGM) led to the disjunctive distribution of *Pedicularis kansuensis* (Orobanchaceae) between the Qinghai-Tibetan plateau and Tianshan region. PLoS ONE, 11(11):online.

DOI: <https://doi.org/10.1371/journal.pone.0165700>

RESEARCH ARTICLE

# Long-Distance Dispersal after the Last Glacial Maximum (LGM) Led to the Disjunctive Distribution of *Pedicularis kansuensis* (Orobanchaceae) between the Qinghai-Tibetan Plateau and Tianshan Region

Wen-Jun Li<sup>1,2</sup>, Xiao-Lin Sui<sup>3</sup>, Patrick Kuss<sup>4</sup>, Yan-Yan Liu<sup>1</sup>, Ai-Rong Li<sup>3\*</sup>, Kai-Yun Guan<sup>1,3\*</sup>

**1** Key Laboratory of Biogeography and Bioresource in Arid Land, Xinjiang Institute of Ecology and Geography, Chinese Academy of Sciences, Urumqi 830011, China, **2** University of Chinese Academy of Sciences, Beijing 100049, China, **3** Yunnan Key Laboratory for Research and Development of Wild Plant Resources, Kunming Institute of Botany, Chinese Academy of Sciences, Kunming 650201, China, **4** Institute of Systematic and Evolutionary Botany, University of Zurich, 8008 Zurich, Switzerland

\* [airongli@mail.kib.ac.cn](mailto:airongli@mail.kib.ac.cn) (ARL); [guanky@mail.kib.ac.cn](mailto:guanky@mail.kib.ac.cn) (KYG)



## OPEN ACCESS

**Citation:** Li W-J, Sui X-L, Kuss P, Liu Y-Y, Li A-R, Guan K-Y (2016) Long-Distance Dispersal after the Last Glacial Maximum (LGM) Led to the Disjunctive Distribution of *Pedicularis kansuensis* (Orobanchaceae) between the Qinghai-Tibetan Plateau and Tianshan Region. PLoS ONE 11(11): e0165700. doi:10.1371/journal.pone.0165700

**Editor:** William Oki Wong, Institute of Botany, CHINA

**Received:** February 25, 2016

**Accepted:** October 17, 2016

**Published:** November 2, 2016

**Copyright:** © 2016 Li et al. This is an open access article distributed under the terms of the [Creative Commons Attribution License](https://creativecommons.org/licenses/by/4.0/), which permits unrestricted use, distribution, and reproduction in any medium, provided the original author and source are credited.

**Data Availability Statement:** All relevant data are within the paper and its Supporting Information files.

**Funding:** This work was supported by the Natural Science Foundation of China (U1303201, 31600447, 31370512, 31400440), a grant from The Youth Innovation Promotion Association of CAS (to ARL), the Stiftung zur Förderung der Pflanzenkenntnis (Basel/CH), and the US National Science Foundation (No. DEB-1119098) (to PK).

## Abstract

Quaternary climate fluctuations have profoundly affected the current distribution patterns and genetic structures of many plant and animal species in the Qinghai-Tibetan Plateau (QTP) and adjacent mountain ranges, e.g. Tianshan (TSR), Altay, etc. In this greater area disjunct distributions are prominent but have nevertheless received little attention with respect to the historical processes involved. Here, we focus on *Pedicularis kansuensis* to test whether the current QTP and TSR disjunction is the result of a recent Holocene range expansion involving dispersal across arid land bridge(s) or a Pleistocene range fragmentation involving persistence in refugia. Two chloroplast DNA spacers were sequenced for 319 individuals from 34 populations covering the entire distribution range of this species in China. We found a total of 17 haplotypes of which all occurred in the QTP, and only five in the TSR. Overall genetic diversity was high ( $H_T = 0.882$ ,  $H_S = 0.559$ ) and higher in the QTP than in the TSR. Genetic differentiation among regions and populations was relatively low ( $G_{ST} = 0.366$ ) and little evidence for a phylogeographic pattern emerged. The divergence times for the four main lineages could be dated to the early Pleistocene. Surprisingly, the two ubiquitous haplotypes diverged just before or around the Last Glacial Maximum (LGM) and were found in different phylogenetic lineages. The Species Distribution Model suggested a disappearance of *P. kansuensis* from the TSR during the LGM in contrast to a relatively constant potential distribution in the QTP. We conclude that *P. kansuensis* colonized the TSR after the LGM. The improbable long-distance dispersal by wind or water across arid land seed flow may well have had birds or men as vector.

**Competing Interests:** The authors have declared that no competing interests exist.

## Introduction

Tectonic events and climate fluctuations have profoundly shaped the current distribution patterns and genetic structures of many plant and animal species in temperate zones of the Northern Hemisphere [1–4]. Since the early Cenozoic, the geology and topography of East Asia underwent dramatic changes. Most notably is the uplift of the Qinghai-Tibetan Plateau (QTP) and adjacent mountain ranges, e.g. Tianshan (TSR) and Altay Mts., which entailed pronounced climatic and environmental dynamics in both space and time [5–7] and a strong effect on landscape and vegetation [8,9]. One consequence is the intense aridification of the Tarim Basin in northwestern China [10–13], resulting in an arid area of about  $6.00 \times 10^5$  km<sup>2</sup> between the QTP and the TSR [14].

The present day distribution of plant and animal species is strongly influenced by these historical processes which potentially and iteratively led to range shifts, range expansion, range contraction and/or range fragmentation. In this context, a disjunct distribution could either be the result of long-distance dispersal from a source area into a suitable new area [15–18] or the consequence of disruption of the previously continuous distribution range [19,20]. Phylogenetic relationship [16–18] and genetic diversity within a given species [21–24] are two aspects frequently considered in order to unravel the historical processes involved. Theoretical and empirical evidence suggests that, when the disjunction is due to recent long-distance dispersal, individuals from separated regions will cluster together in a phylogenetic tree [16–18]. Additionally, the regions are characterized by different levels of genetic diversity [23,25] with the newly colonized region harboring lower levels. By contrast, in the case of range fragmentation, individuals from different regions will cluster by region [18,23] while levels of genetic diversity remain comparable [19,20,24]. Obviously, the level and spatial distribution of genetic diversity within a species is also dependent on the combination of life-history traits, e.g. longevity, breeding system [26,27], which can mask the genetic imprint of historical processes.

Although numerous phylogeographical studies have been carried out in either the QTP [4,28,29] or the greater Tianshan-Altay region [19,21,30–34], investigations addressing the historical processes that led to disjunct distributions are scarce. The limited data available show that plant species had low genetic diversity in Tianshan-Altay region, indicating a rapid colonization from the QTP and strong founder effects in the Tianshan-Altay region [35–37]. However, these studies included either samples from only one Altay population, i.e. the congeneric *Pedicularis longiflora* [35], or plant species less representative of highland terrestrial plants, i.e. the fern *Lepisorus clathratus* and the aquatic *Hippuris vulgaris* [36,37]. Thus, it remains questionable whether the current QTP and TSR disjunctions are the result of a recent Holocene range expansion involving dispersal across arid land bridge(s) or a Pleistocene range fragmentation involving persistence in refugia.

Here, we focus on *Pedicularis kansuensis* Maxim. (Orobanchaceae), a highland plant species widespread in western China and Nepal, with a disjunct distribution between the QTP and the TSR but not known from the Altay. This species was previously mis-identified as *P. verticillata* in the TSR [38–41], but clarified to be *P. kansuensis* based on morphological and molecular evidence [42]. It is an annual or facultative biennial hemiparasitic herb, occurring in moist gravelly ground or grassy slopes in subalpine zone at elevations between 1,800 and 4,600 m [43]. In nearly twenty years, *P. kansuensis* has been reported to rapidly expand in population sizes and become weedy in Bayanbulak Grassland of the Tianshan Mts., which has caused great loss of herbage yield and threatened the local livestock industry [39,44].

In the present study we aim to unravel the historical processes that led to the current disjunctive distribution of *P. kansuensis*. Given the great extent of today's arid Tarim Basin which separate the QTP and the TSR we propose two alternative scenarios: (a) *P. kansuensis* survived

the LGM *in situ* or in refugia in the respective foothills. Here we would expect a strong phylogeographic signal, existence of unique regional haplotypes and comparable high levels of genetic diversity. (b) *P. kansuensis* colonized the TSR from the northern fringes of the QTP via long-distance seed dispersal after the LGM. Under this scenario we would expect to find a certain degree of genetic similarity between the source and sink regions, i.e. shared haplotypes, but not a strong phylogeographic signal. Also, the sink region would be characterized by lower levels of genetic diversity and evidence for rapid population expansion should be detectable.

## Materials and Methods

### Ethics statement

This study was conducted in accordance with the laws of the People's Republic of China. No specific permits were required for accessing the sampling locations. *P. kansuensis* is not an endangered or protected species.

### Plant sampling

Leaf tissue of *P. kansuensis* was collected from 34 populations across the Qinghai-Tibetan Plateau (QTP) and the Tianshan region (TSR) in western China (Table 1). Three to 16 individuals growing at least 20 m apart were sampled in each georeferenced population rendering a total of 319 individuals. Fresh leaves were dried in silica gel and stored at room temperature until DNA extraction. For all populations voucher specimens were deposited at the Herbarium of the Xinjiang Institute of Ecology and Geography, Chinese Academy of Sciences, Xinjiang, China (XJBI) (S1 Table).

### DNA extraction, amplification and sequencing

Genomic DNA was extracted using a Plant Genomic DNA Isolation kit (Tiangen, Beijing, China) following the manufacturer's instructions. The *trnL-trnF* [45] and *rpl32-trnL* [46] intergenic regions, widely used in plant phylogeographical analyses [21,30,32], were amplified and sequenced. PCR reactions were carried out in a total volume of 25  $\mu$ L containing 20 ng template DNA, 2.5  $\mu$ L PCR buffer, 2  $\mu$ L  $MgCl_2$  (25 mmol/L), 0.5  $\mu$ L dNTP mix (2.5 mmol/L), 1  $\mu$ L each primer (5 pmol/L), and 0.3  $\mu$ L (1 unit) Taq DNA polymerase. For DNA amplification a T1 thermo-cycler (Biometra, Göttingen, Germany) was used with an initial denaturation at 94°C for 3 min, followed by 32 cycles of denaturation at 94°C for 30 s, annealing at 53°C for 45 s, extension at 72°C for 1 min, and a final extension of 10 min at 72°C. The PCR products were checked on a 1.0% agarose gel, and then bidirectionally sequenced in a commercial laboratory (Sangon, Shanghai, China) following standard sequencing protocols.

### Genetic diversity and population structure

Chloroplast DNA (cpDNA) sequences were aligned with CLUSTAL W [47] and postprocessed manually. Insertions/deletions (indels) were coded as point mutations and received equal weight to other mutations. Chloroplast DNA haplotypes were identified based on variations in the aligned sequences of the *trnL-trnF* and *rpl32-trnL* spacers using DnaSP ver. 5.0 [48]. All of the cpDNA non-coding region of each chloroplast haplotype and outgroup were deposited in GenBank with the accession numbers KX180093-KX180130 (S1 Table). Haplotype diversity (*h*) and nucleotide diversity ( $\pi$ ) for each population, for groups of populations and for all populations were calculated in ARLEQUIN 3.5 [49]. The effect of unequal sample sizes was assessed by rerunning analyses with alternative input files created through multiple random reductions

**Table 1. Details of sample locations, samples size (N), haplotypes, haplotype diversity (h) and nucleotide diversity ( $\pi$ ) of 34 populations of *Pedicularis kansuensis* surveyed for DNA sequence variation at two combined chloroplast regions.**

Population code	Sample location	Coordinates (N/E)	Altitude (m)	N	Haplotypes	h (S $\pm$ D)	$\pi$ (S $\pm$ D) $\times 10^{-3}$
TSG	Tianshan group			42	5	0.718 $\pm$ 0.042	10.393 $\pm$ 5.243
BLK	Balikun, XJ	43°21′/93°42′	2085	14	H1,H2,H3,H4,H5	0.736 $\pm$ 0.107	6.989 $\pm$ 3.793
BY	Bayanbulak, XJ	42°84′/83°72′	2458	11	H1,H2,H3	0.618 $\pm$ 0.104	10.575 $\pm$ 5.757
HM	Hami, XJ	43°15′/93°38′	1921	8	H2	0	0
WLMQ	Urumqi, XJ	43°11′/86°85′	2031	9	H1,H2,H4,H5	0.750 $\pm$ 0.112	7.053 $\pm$ 4.015
QTPG	Qinghai-Tibetan Plateau group			277	17	0.889 $\pm$ 0.011	7.344 $\pm$ 3.690
SN1	Sunan, GS	39°02′/99°28′	2497	13	H1,H3,H5	0.641 $\pm$ 0.097	3.161 $\pm$ 1.845
SN2	Sunan, GS	38°3′/100°25′	2445	10	H4	0	0
TJ	Tianjun, QH	37°05′/98°52′	2533	16	H1,H2,H4,H5,H14	0.825 $\pm$ 0.045	9.183 $\pm$ 4.862
QL	Qilian, QH	38°05′/100°2′	2972	8	H1,H2,H3,H7	0.750 $\pm$ 0.139	9.113 $\pm$ 5.211
GC	Gangcha, QH	37°2′/100°31′	3428	12	H1,H2,H4,H5,H14	0.727 $\pm$ 0.113	8.983 $\pm$ 4.880
DT	Datong, QH	37°17′/101°24′	3712	14	H1,H2,H4,H7	0.692 $\pm$ 0.094	4.282 $\pm$ 2.408
HY	Huangyuan, GS	36°25′/101°13′	3375	10	H1,H4,H5,H7,H14	0.844 $\pm$ 0.080	3.101 $\pm$ 1.864
CD1	Chengduo, GS	33°21′/97°08′	4500	7	H1	0	0
XH1	Xunhua, QH	35°36′/102°41′	2792	8	H1,H3	0.536 $\pm$ 0.123	3.017 $\pm$ 1.876
SD	Shandan, GS	38°27′/101°11′	2358	15	H1,H3,H5	0.629 $\pm$ 0.086	3.206 $\pm$ 1.846
TZ	Tianzhu, GS	37°09′/102°5′	2613	11	H1,H2,H13	0.473 $\pm$ 0.162	4.304 $\pm$ 2.476
LT1	Lintan, GS	34°41′/103°34′	2800	7	H6,H7,H15	0.714 $\pm$ 0.127	10.019 $\pm$ 5.841
ZK1	Zeku, QH	35°18′/101°56′	2824	10	H1,H7,H14	0.689 $\pm$ 0.104	2.033 $\pm$ 1.293
ZK2	Zeku, QH	35°05′/101°36′	3426	10	H1	0	0
LX	Linxia, GS	35°34′/102°46′	3175	3	H1	0	0
GD	Gande, QH	34°00′/100°02′	4153	4	H1,H5,H7	0.833 $\pm$ 0.222	1.566 $\pm$ 1.261
LT	Litang, SC	30°1′/99°58′	3656	9	H1,H2,H4,H11,H12	0.833 $\pm$ 0.098	7.795 $\pm$ 4.413
KD	Kangding, SC	30°02′/101°3′	4346	8	H1,H11	0.536 $\pm$ 0.123	0.336 $\pm$ 0.352
DG	Dege, SC	31°41′/98°33′	3162	10	H1,H7,H9,H10,H17	0.867 $\pm$ 0.071	5.705 $\pm$ 3.246
DC	Daocheng, SC	29°07′/100°12′	3778	8	H6,H7	0.536 $\pm$ 0.123	1.007 $\pm$ 0.756
JD	Jiangda, XZ	31°32′/98°2′	3440	11	H2,H7,H10,H17	0.491 $\pm$ 0.175	5.507 $\pm$ 3.106
GZ	Ganzhi, SC	31°38′/99°48′	3385	6	H1,H10	0.333 $\pm$ 0.215	0.418 $\pm$ 0.425
YJ	Yajiang, SC	30°00′/100°4′	4173	7	H1,H2,H4,H9,H11	0.905 $\pm$ 0.103	7.832 $\pm$ 4.618
DZ	Dazhi, XZ	29°46′/91°50′	3910	10	H2,H7	0.467 $\pm$ 0.132	8.766 $\pm$ 4.866
MK	Mangkang, ZX	29°27′/98°38′	3681	6	H2,H8,H12	0.600 $\pm$ 0.215	6.345 $\pm$ 3.908
DQ	Dingqing, XZ	31°06′/96°21′	4321	10	H2,H6,H7,H8,H9	0.756 $\pm$ 0.130	9.109 $\pm$ 5.047
SD2	Songduo, XZ	29°52′/92°31′	4231	6	H1,H7	0.333 $\pm$ 0.215	0.209 $\pm$ 0.275
CD2	Changdu, XZ	31°21′/97°29′	3730	7	H1,H9,H16	0.667 $\pm$ 0.160	11.211 $\pm$ 6.508
SX	Suoxian, XZ	31°48′/93°43′	3979	12	H9,H12,H15,H17	0.455 $\pm$ 0.170	4.523 $\pm$ 2.567
NQ	Naqu, XZ	31°44′/92°39′	4432	9	H9,H12,H15,H16	0.778 $\pm$ 0.110	10.604 $\pm$ 5.919
<b>Total</b>				319	17	0.882 $\pm$ 0.010	8.010 $\pm$ 4.004

Abbreviation of Chinese Provinces: GS-Gansu, QH-Qinghai, SC-Sichuan, XJ-Xinjiang, XZ-Xizang (Tibet).

doi:10.1371/journal.pone.0165700.t001

[50] scripted in R ver. 3.2.3 [51]. No significant differences between the curtailed and the full data set were found so that we decided to proceed with analysis of the full dataset.

SAMOVA ver. 1.0 was used to investigate the spatial component in the dataset by defining  $K$  groups of populations that are geographically homogeneous and genetically differentiated from each other (10,000 iterations; range of  $2 \leq K \leq 10$ ) [52]. The result file, a pairwise cpDNA  $F_{ST}$  distance matrix, was imported into BARRIER [53] which incorporates Monmonier's maximum-

difference algorithm [54] to visualize the geographic location of genetic breaks among (groups of) populations. Using this method, we divided the distribution range of *P. kansuensis* populations into two groups, Tianshan group (TSG) and QTP group (QTPG). Furthermore, isolation by distance (IBD) [55], the correlation between genetic and geographical distance was checked with a Mantel test [56] using ALLELES IN SPACE (AIS) [57]. Genetic structure was assessed with an Analysis of Molecular Variance (AMOVA) [58] in ARLEQUIN 3.5 [49] with significance tests based on 10,000 permutations. Parameters of within-population gene diversity ( $H_S$ ), total gene diversity ( $H_T$ ), and genetic differentiation ( $G_{ST}$ ,  $N_{ST}$ ) were estimated according to Pons and Petit [59]. Significant phylogeographic structure was inferred by testing whether  $N_{ST}$  was significantly greater than  $G_{ST}$  using U-statistic. If  $N_{ST}$  is significantly higher than  $G_{ST}$ , closely related haplotypes occur more often in the same populations than less closely related haplotypes, indicating the presence of phylogeographical structure [59].

## Phylogenetic relationship and divergence time

Phylogenetic relationships among *P. kansuensis* cpDNA haplotypes were analyzed using Neighbor-joining (NJ), Maximum parsimony (MP) and Maximum Likelihood (ML) algorithms implemented in MEGA ver. 6.0 [60], with *P. violascens* and *P. verticillata* as outgroups. Gaps in sequences were treated as the fifth character state. We constructed MP trees using a heuristic search with 1,000 random additions of sequences and tree-bisection reconnection (TBR) branch swapping. The ML and MP trees were computed with 1,000 bootstrap replicates in Kimura's two-parameter model. Furthermore, NETWORK ver. 4.6 [61] was used to construct median-joining networks to detect genealogical relationships among the haplotypes of *P. kansuensis*. The gaps were treated as a single mutation event.

Divergence times for different *P. kansuensis* lineages were estimated through a Bayesian approach implemented in BEAST ver. 1.8.1 [62]. In running MODELTEST ver. 3.7 [63], generalized time reversible (GTR) substitution model and Gamma site heterogeneity model were selected as the best-fit nucleotide substitution model for our dataset of aligned sequences. Due to a lack of fossils of *P. kansuensis* or its congeneric relatives, substitution rates were used for approximate divergence times. For most angiosperms, the cpDNA substitution rates are estimated to vary between 1.0 and  $3.0 \times 10^{-9}$  substitutions per site per year [s/s/y], while  $8.24 \times 10^{-9}$  for *trnL-trnF* [64]. Because *P. kansuensis* is an annual or biennial herb and *trnL-trnF* was used in this study, the value of 3.0 and  $8.24 \times 10^{-9}$  was specified in BEAST with an additional uncorrelated lognormal relaxed molecular clock assumption. The Markov chain Monte Carlo (MCMC) chains were run for 10,000,000 generations, sampling every 1,000 generations. The combined parameters were checked in TRACER ver. 1.5 [65]. The Bayesian trees were combined and annotated by TREE ANNOTATOR ver. 1.8.1 (part of the BEAST 1.8.1 package).

## Population demographic analyses

To investigate whether populations or groups of populations experienced any population expansion, Tajima's  $D$  [66] and Fu & Li's  $D^*$  [67] were calculated using ARLEQUIN 3.5 [49]. In addition, mismatch distribution analysis was also calculated in ARLEQUIN with 1,000 parametric bootstrap replicates. The sum of squared deviations (SSDs) between observed and expected mismatch distribution were computed and  $P$  values were calculated as the proportion of simulations producing a larger SSD than the observed SSD. The raggedness index ( $HR_{ag}$ ) and its significance were also calculated to quantify the smoothness of the observed mismatch distribution [68].



## Species distribution modelling

Lastly, in order to estimate the current potential distribution range of *P. kansuensis* as well as during the Last Glacial Maximum (LGM; 21 ka before present), a species distribution model (SDM) was computed using the maximum entropy algorithm implemented in MAXENT 3.3.1 [69]. Present day climate data available from the World Clim database (34 stations, 19 bioclimatic variables, 2.5 arcmin resolution) [70] (available at <http://www.worldclim.org/download>) along with 34 tested geographical data produced by ourselves were used to estimate the present potential distribution range. The community climate system model (CCSM) [71] was then employed to generate the potential distribution during the LGM. To test the reliability of the results, goodness of fit between the model and the training data was assessed by analyzing the area under the receiver operating characteristic curve (AUC). Finally, a jackknife test was performed to measure the relative importance of climatic variables on the occurrence prediction for every distribution model.

## Results

### Chloroplast variation and haplotype distribution

The aligned sequences of *trnL-trnF* and *rpl32-trnL* were 830 bp and 770 bp in length, respectively, with a total length of the combined alignments of 1,600 bp. Variable sites showed 40 substitutions and 15 indels. In total, 17 haplotypes (H1-H17) were identified (Fig 1, Table 1). Among these, H1 and H2 were widespread haplotypes, occurring in 23 (67.65%) and 16 (47.06%) populations, respectively. All 17 haplotypes were found in the QTP and only five in the TSR (H1-H5). Thus, no haplotype was exclusive for the TSR. Population contained a maximum of five haplotypes and a minimum of one. There was no significant correlation between the number of sampled individuals per population and the number of haplotypes ( $R = 0.3$ ;  $P > 0.05$ ).

### Genetic diversity and structure

Haplotype diversity ( $h$ ) ranged from 0.000 to 0.905 and the YJ (Yajiang) population in the Sichuan Hengduan Mts. contributed the highest value (Table 1, Fig 1). Nucleotide diversity ( $\pi$ ) varied between 0.000 and  $11.210 \times 10^{-3}$  with a maximum present in the CD2 (Changdu) population in SE Tibet (Table 1, Fig 1). Total genetic diversity based on haplotype variation across all populations was  $H_T = 0.882$  and the average within-population diversity was  $H_S = 0.559$  (Table 2).

The permutation test showed that there was no significant difference between  $G_{ST} = 0.366$  and  $N_{ST} = 0.376$  ( $U = 0.11$ ;  $P > 0.05$ ). Thus, the hypothesis of a strong phylogeographic pattern was rejected. In the SAMOVA analyses,  $F_{CT}$  values decreased progressively as the values for  $K$  number of groups increased from 2 to 10 with no unambiguous number of  $K$  supported. Also here the hypothesis of a phylogeographic pattern was rejected. Furthermore, the Mantel test revealed a significant correlation between genetic and geographical distances ( $R = 0.127$ ,  $P < 0.001$ ) over all populations. However, a genetic break (barrier) separating the TSR populations from those of the QTP was found with a robustness of 90% (Fig 2). This barrier corresponds to the arid land between the two disjunctive geographic regions. Hierarchical analysis of molecular variance (AMOVA) showed that a low variation (2.52%) was partitioned to the two putative groups of populations, while 33.03% and 64.44% variation was partitioned among populations within groups and within populations, respectively (Table 3).

### Phylogenetic and genealogical relationships of cpDNA haplotypes

The topology of the Neighbor-joining (NJ) tree calculated for 17 haplotypes from 319 *P. kansuensis* individuals is shown in Fig 3. Four clades were strongly supported ( $\geq 94\%$  bootstrap

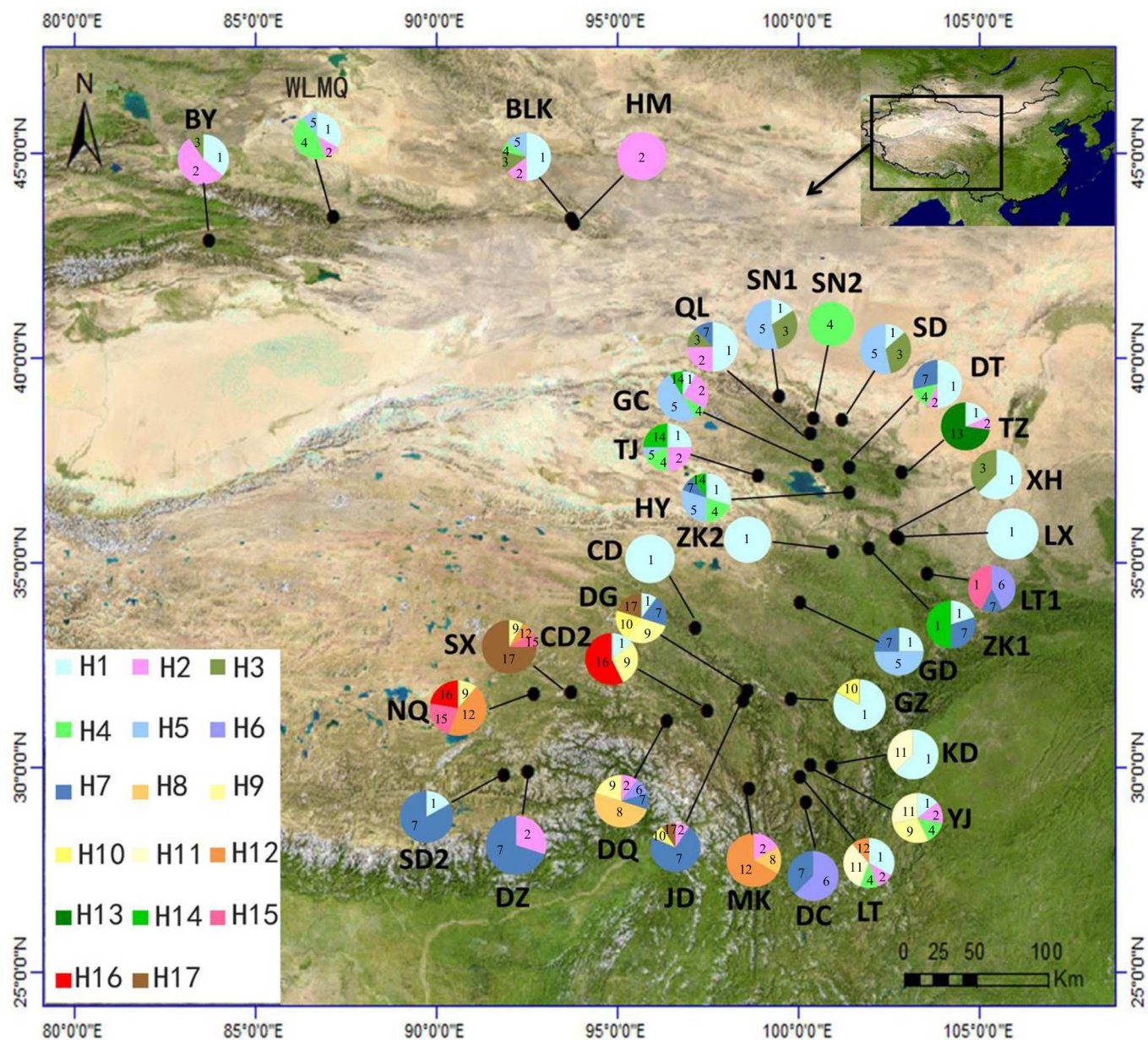


**Fig 1. Sample sites (population codes as in Table 1) and geographic distribution of chloroplast DNA (cpDNA) haplotypes (H1-H17) detected in 34 populations of *Pedicularis kansuensis* in the Qinghai-Tibetan Plateau (QTP) and the Tianshan region (TSR). Pie charts show the different haplotypes and their frequency in each population.**

doi:10.1371/journal.pone.0165700.g001

support). The haplotypes in clade I and II mainly occurred in populations from the SE of the QTP with the exception of H2, a widespread haplotype present in 16 populations. Clade IV contained four haplotypes which all stem from the NE edge of the QTP and the TSR. Clade III was the most complicated one, containing 7 haplotypes distributed in 33 populations. Among these haplotypes, H1 represented the most widespread haplotype in our study, occurring in 23 populations. H9-H11 were found in the SE of the QTP. H5 was found in the NE of the QTP and in the TSR. The results of the median-joining network obtained by NETWORK ver. 4.6 [61] showed the same phylogenetic relationship as those revealed by the NJ tree (Fig 3). Also,



**Table 2. Estimates of average gene diversity results for *Pedicularis kansuensis* within regions.**

Region	$H_S$	$H_T$	$G_{ST}$	$N_{ST}$
All data	0.559 ±0.047	0.882 ±0.025	0.366 ±0.050	0.376 ±0.069
Tianshan group	0.526 ±0.178	0.753 ±0.109	0.301 ±0.225	0.481 ±0.269
QTP group	0.556 ±0.051	0.880 ±0.029	0.368 ±0.051	0.386 ±0.074

Abbreviations:  $H_S$ —average gene diversity within populations;  $H_T$ —total gene diversity;  $G_{ST}$ —inter population differentiation;  $N_{ST}$ —number of substitution types.

doi:10.1371/journal.pone.0165700.t002

the maximum parsimony (MP) and maximum likelihood (ML) trees were essentially identical to the NJ tree with respect to the major clades and were thus not shown here.

### Lineage divergence time and population spatial expansion

Divergence times between the haplotypes ranged from 2.339 to 0.034 Mya when the value of  $3.0 \times 10^{-9}$  s/s/y was specified in BEAST, while 0.885 to 0.012 Mya for  $8.24 \times 10^{-9}$  s/s/y (Fig 3).

The mismatch distribution for pairwise differences over all populations and two geographical

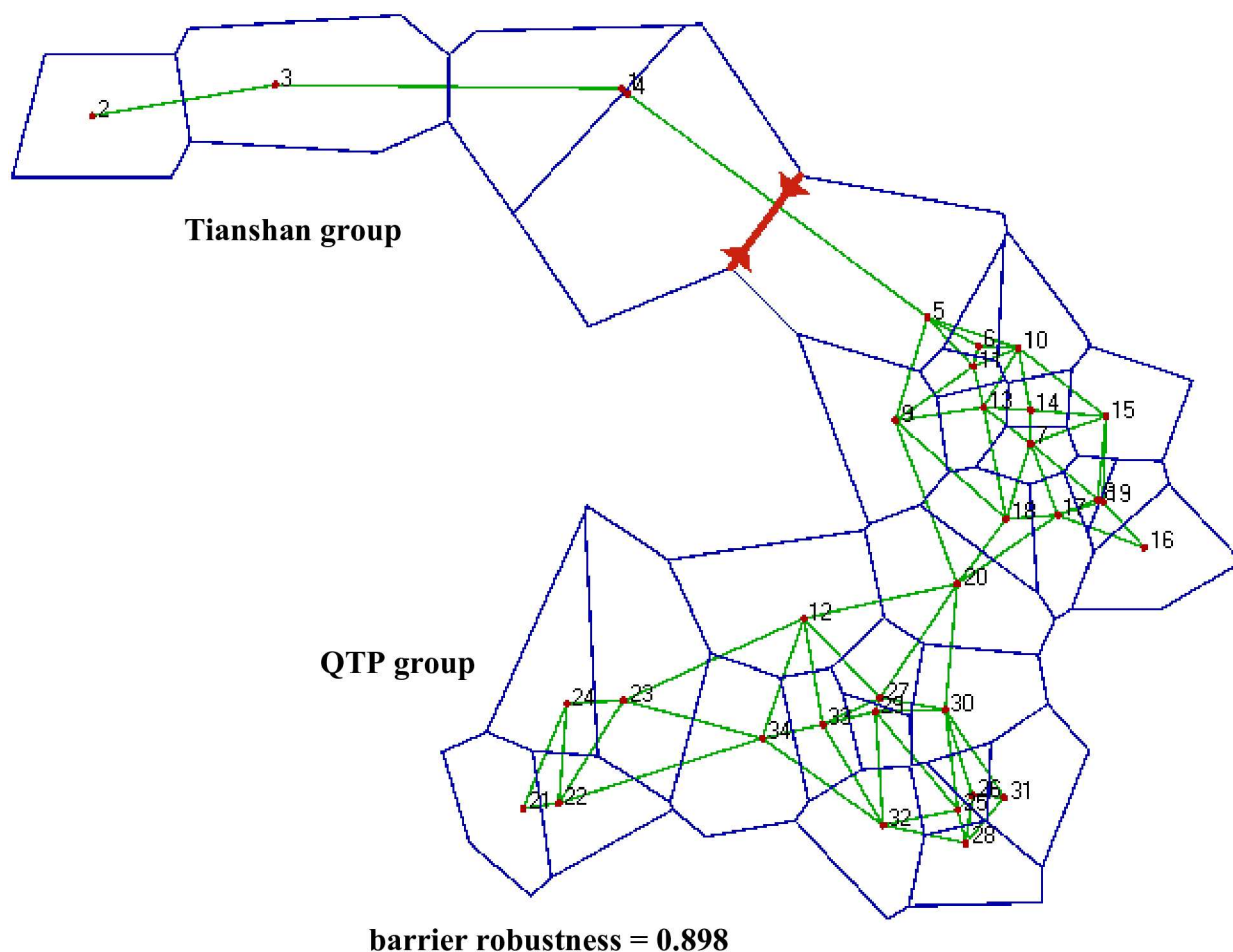


**Fig 2. Location of inter-population genetic breaks in *Pedicularis kansuensis* in the Qinghai-Tibetan Plateau (QTP) and Tianshan region (TSR).** Outlines represent the polygons of the Voronoi tessellation with the centers of the populations omitted. Red line represent the barrier. The distribution range of *P. kansuensis* was divided into two groups, Tianshan group (TSG) and QTP group (QTPG).

doi:10.1371/journal.pone.0165700.g002

**Table 3. Analysis of molecular variance for 34 sampled populations of *Pedicularis kansuensis* based on two cpDNA spacer sequence data.**

Source of variation	d.f.	Sum of squares	Variance components	Percentage of variation	Fixation Index
Among groups	1	2.763	0.01146	2.52	$F_{SC}$ : 0.33886
Among pops. within groups	32	54.029	0.14998	33.03	$F_{ST}$ : 0.3555
Within pops.	285	83.397	0.29262	64.44	$F_{CT}$ : 0.02525
Total	318	140.188	0.45895		

Abbreviation: d.f.—degrees of freedom.  $F_{CT}$ —correlation of chlorotypes within groups relative to the total;  $F_{SC}$ —correlation within populations relative to groups;  $F_{ST}$ —correlation within populations relative to the total.

doi:10.1371/journal.pone.0165700.t003

groups were clearly multimodal (Fig 4), indicating that this species has not experienced a sudden expansion. This was corroborated by positive and insignificant Tajima's  $D$  and Fu & Li's  $D^*$  tests (Table 4).

### Species distribution modeling

The 'area under the curve' (AUC) values for the training and the test data of *P. kansuensis* amounted to 0.998 and 0.995, respectively, indicating good performance of the present-day

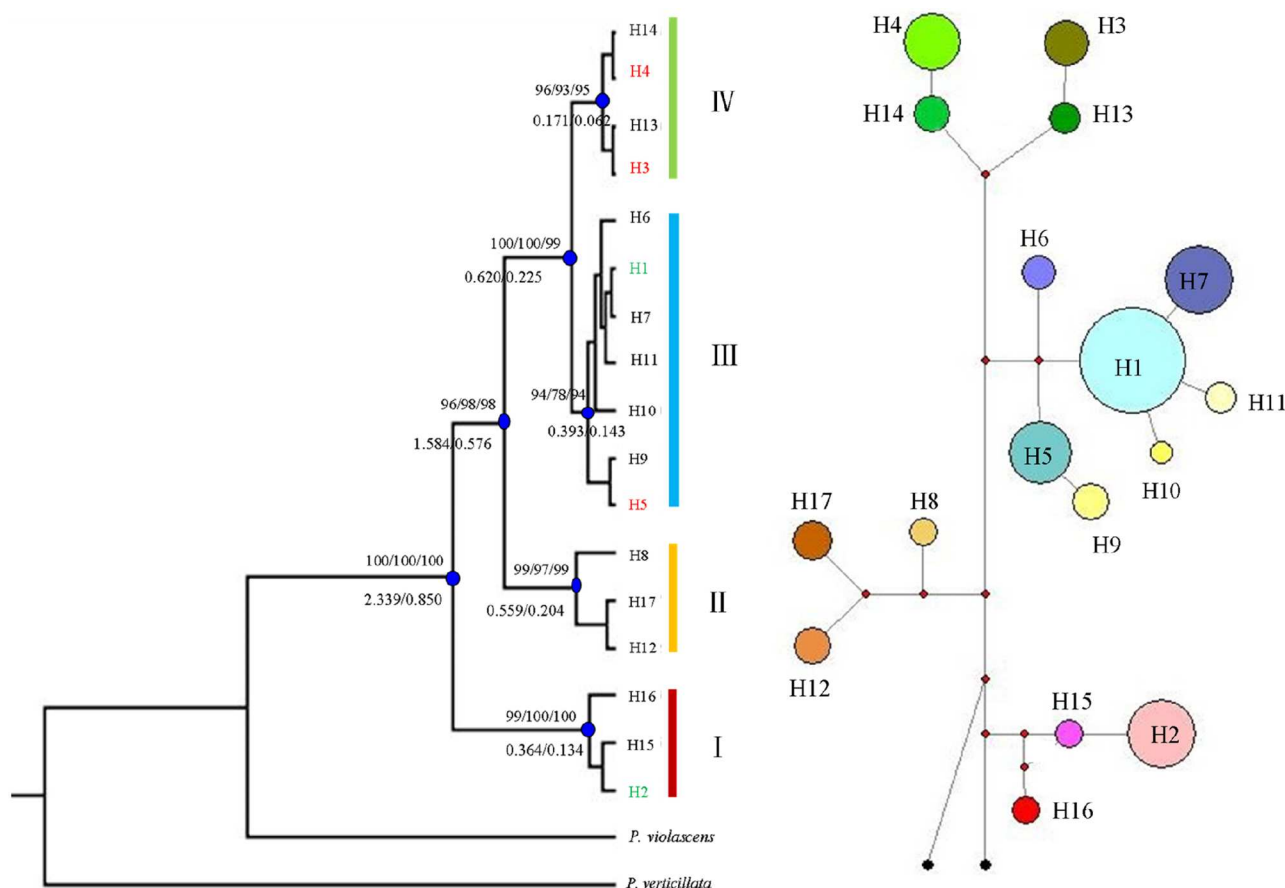


**Fig 3. The NJ tree topology (left) and network (right) of the 17 cpDNA haplotypes detected in *Pedicularis kansuensis* and their divergence times estimated with the average evolutionary rate based on BEAST analysis.** The values above the branch represent the bootstrap values for NJ (left), MP (middle) and ML (right) analyses, respectively. The values under the branching represent the divergence time (in million years ago), based on  $3.0 \times 10^{-9}$  substitutions per site per year [s/s/y] and  $8.24 \times 10^{-9}$  s/s/y. The circle sizes in the network are proportional to haplotype frequency, and the black points represent outgroups.

doi:10.1371/journal.pone.0165700.g003

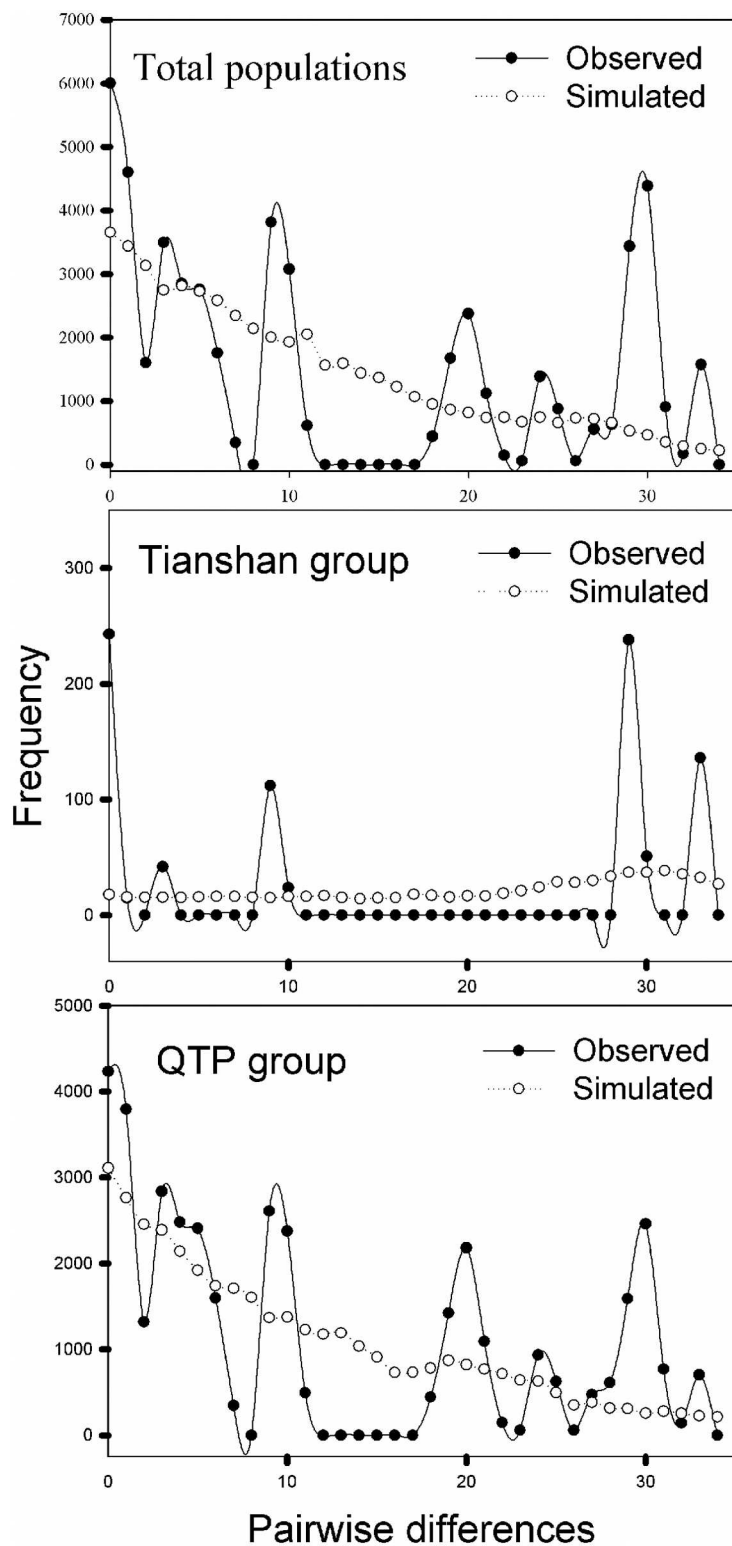


**Fig 4.** Mismatch distribution analysis of cpDNA sequence data from all sampled populations in the Qinghai-Tibetan Plateau group (QTPG) and the Tianshan group (TSG).

doi:10.1371/journal.pone.0165700.g004

**Table 4. Parameters of mismatch distribution analyses, Tajima's D and Fu & Li's D\* tests.**

Groups	Mismatch distribution analyses		Tajima's D test ( <i>P</i> )	Fu & Li's D* tests ( <i>P</i> )
	SSD ( <i>P</i> <sub>SSD</sub> )	HRag ( <i>P</i> <sub>HRag</sub> )		
Total	0.024(0.500)	0.028(0.120)	1.310(0.906)	16.720(0.982)
Tianshan group	0.096(0.120)	0.280(0.390)	3.126(0.999)	21.651(1.000)
QTP group	0.015(0.640)	0.022(0.510)	0.856(0.814)	13.363(0.999)

Abbreviations: HRag (*P*<sub>HRag</sub>)—raggedness statistic (probability of raggedness statistic); SSD (*P*<sub>SSD</sub>)—sum of the square deviations (probability of sum of the square deviations).

doi:10.1371/journal.pone.0165700.t004

distribution range and the Last Glacial Maximum community climate system model (LGM-CCSM) as visualized in Fig 5. The current potential distribution range of *P. kansuensis* included the east of the QTP as well as the TSR, coinciding well with the species' extant distribution. By contrast, the predicted distribution for the LGM showed occurrences only in the east of the QTP.

## Discussion

### Genetic Diversity and Genetic Structure

In this study, we detected 17 haplotypes from 319 *P. kansuensis* individuals belonging to 34 populations in the QTP and the TSR. In comparison with *P. longiflora*, a congeneric species of *P. kansuensis* which shares many life-history traits (e.g. annual/biennial, insect-pollinated, out-crossing, mid-successional) and has an almost matching distribution range on the QTP with northernmost occurrences in either the Tianshan or the Altay Mts. [43,72,73], the haplotype diversity was slightly higher in *P. kansuensis* ( $H_T = 0.882$  vs.  $H_T = 0.770$ ), though the number of haplotypes found was less than that in *P. longiflora* (30 haplotypes, 41 populations, 910 individuals) [35]. When compared with less related plant species studied in both the QTP and the Tianshan region, haplotype diversity of *P. kansuensis* was also higher (e.g. *Aconitum gymnantrum*

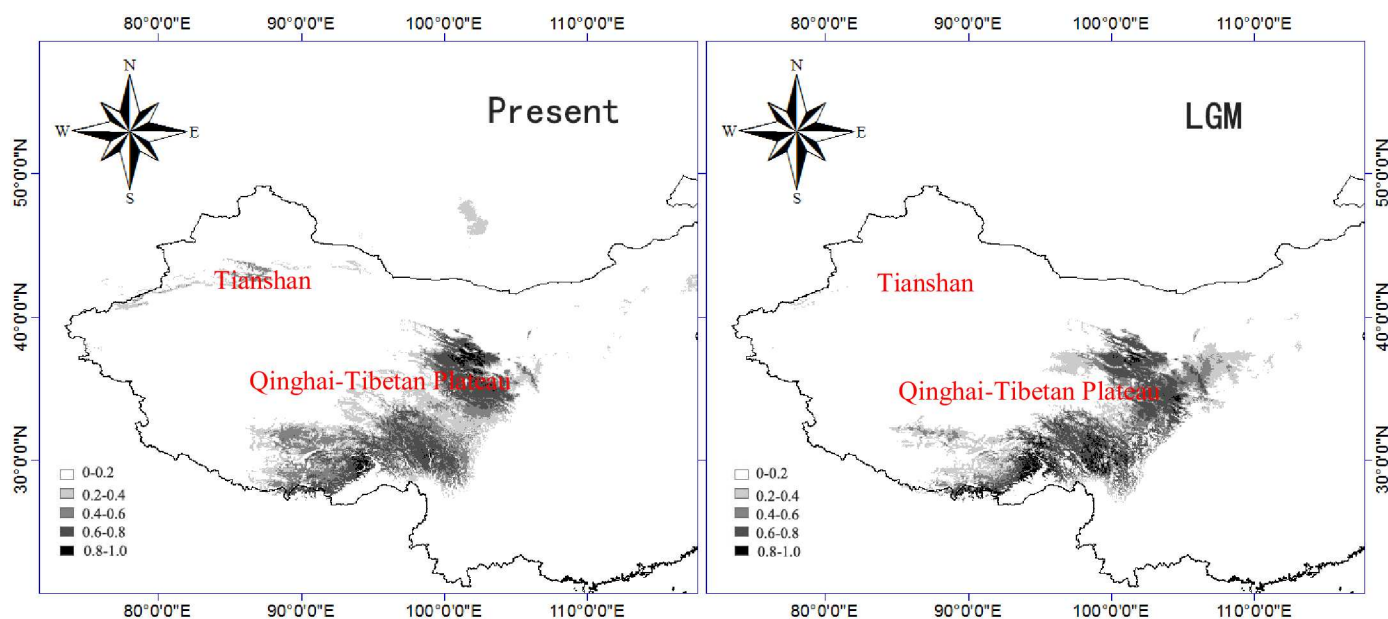


**Fig 5. Potential distribution range for *Pedicularis kansuensis* under current climate conditions (left) and during the Last Glacial Maximum (LGM; right) based on the community climate system model (CCSM).**

doi:10.1371/journal.pone.0165700.g005



( $H_T = 0.739$ ) [74], *Angelica nitida* ( $H_T = 0.818$ ) [75], *Cupressus* spp. ( $H_T = 0.249$  to  $H_T = 0.791$ ) [76], *H. vulgaris* ( $H_T = 0.604$ ) [37], *Juniperus sabina* ( $H_T = 0.57$ ) [21] and the Chinese populations of *Ligularia hodgsonii* ( $H_T = 0.869$ ) [77]). This comparison still holds true when only haplotype diversity of populations from the TSR are considered (Tables 1 and 2) [35–37], despite the fact that *P. kansuensis* haplotype diversity was lower in the TSR than in the QTP ( $H_T = 0.753$  vs.  $H_T = 0.880$ ). Unlikely, the high level of total genetic diversity can be attributed to a short life-history trait such as longevity or the outcrossing breeding system of *P. kansuensis*. Considerable gene flow among populations and regions may have played a role in shaping the genetic structure, as deduced from the low levels of genetic differentiation among populations in the entire study area ( $G_{ST} = 0.366$ ), the QTP ( $G_{ST} = 0.368$ ), or the TSR ( $G_{ST} = 0.301$ ) (Table 2).

Gene flow of cpDNA is only possible via means of seeds or clonal plant fragments. [78,79]. In the absence of asexual means for reproduction in *P. kansuensis*, our results, i.e. high genetic diversity within population and low population differentiation, suggest relatively frequent seed exchange among populations. The seeds of *P. kansuensis*, however, have no obvious morphological adaptations to wind, water or animal dispersal [80,81]. Nevertheless, water flow has been shown to be an effective way of seed dispersal for *P. kansuensis* [82], but the hydrography of the Tarim Basin makes this option improbable. Also, secondary wind dispersal across frozen land surfaces seems unlikely given the elevational gradients and northerly winter wind direction [83]. Animal activities, especially migratory birds, as well as transportation of contaminated herbage seeds may have played a role in the dispersal of seeds across the Tarim Basin [84–86] despite the fact that direct observations are lacking. These latter two options could well explain why we did not find a strong phylogeographic signal with a clear separation of populations from the QTP and the TSR. The SAMOVA results rendered no support for a distinct number of  $K$  groups of populations, the comparison of  $G_{ST}$  and  $N_{ST}$  values showed no significant difference (Table 2;  $U = 0.11$ ;  $P > 0.05$ ) and only 2.52% of the molecular variance could be contributed to differences among the two regions (Table 3). The genetic barrier is thus very weak despite being detected with high robustness (Fig 2) in BARRIER. Just like the limited available studies of species with a similar distribution pattern, we found no convincing evidence for genetic differentiation in *P. kansuensis* between the QTP and the TSR [35–37].

## Extensive survival in the QTP through the Quaternary

The divergence of all *P. kansuensis* haplotypes could be dated back to 2.339 (0.850) Mya time window that coincides with the early or middle Pleistocene, suggesting that *P. kansuensis* withstood the extensive climate changes during the Quaternary. During this period, the QTP had experienced four major glaciations [87] and several glacial and interglacial cycles [88]. Based on the estimated divergence times of main lineages and most of the haplotypes, we presume that the Quaternary climatic oscillations may have greatly shifted distribution range of *P. kansuensis* in the QTP, affected its divergence events, and shaped its phylogeographic structure, just as reported in other plant species [1–4,28,29,89]. Based on recent phylogeographical studies in the demographic history of plant species from the QTP, two main refugium hypotheses have been proposed. One hypothesis suggested some species may have retreated to the eastern or south-eastern plateau edge (e.g. Hengduan Mts.) as refugia during the Quaternary glacial periods, and then recolonized QTP and its surrounding regions during the interglacial phases or at the end of the Last Glacial Maximum (LGM) [35,90–95]. While the other hypothesis suggested some species may have also survived at QTP and its surrounding regions *in situ* through the Quaternary [96,97]. Previous studies in NW China showed species survival in East Tianshan Mountains [22] and Ili (Yili) Valley [33] during the Quaternary. Refugia are usually

correlated with high levels of genetic diversity and unique haplotypes [98]. In this study, H1 and H2 were widespread haplotypes, occurred in 23 (67.65%) and 16 (47.06%) populations, respectively. Some haplotypes (e.g. H8, H9, H10, H11, H15, H16, and H17) occurred in the SE QTP, Hengduan-Himalayan Mts. While H3, H5, H13, and H14 occurred in the NE QTP (e.g. Qilian Mts.) and Tianshan Mts. It seems that *P. kansuensis* might have survived in known refugial areas at SE QTP (e.g. Hengduan Mts.) and the edge of NE QTP (e.g. Qilian Mts.). However, the results of mismatch analyses (Fig 3) and Tajima's  $D$  and Fu & Li's  $D^*$  tests (Table 3) indicated that recent range expansion was rejected, given that *P. kansuensis* survived extensively in the plateau during the LGM. This was also confirmed by the results of SDM that the LGM potential distributions did not show obviously shrink in the QTP in comparison with the current distributions (Fig 5).

### Long-distance dispersal from the QTP to the TSR after the LGM

In this study, all 17 detected haplotypes were found in the QTP, while only five (H1-H5) in the TSR (Fig 1). All five haplotypes (H1-H5) found in the TSR also occurred in NE of the QTP, of which H1 and H2 were widespread over the entire distribution range (Fig 1). In the phylogenetic tree, neither the five (H1-H5) nor the three (H3-H5) haplotypes formed a single clade, but rather clustered with other haplotypes (Fig 3). The divergence time of H1-H5 corresponded to the divergence time of all haplotypes and was dated back to the early Pleistocene, at 2.339 (0.850) Mya, while the one for H3-H5 to 0.620 (0.225) Mya, and H3 and H4 to 0.17 (0.062) Mya. Furthermore, a wide arid region barrier between the TSR and the QTP had developed and aridification begun by the early Pleistocene [99]. The divergence times of the shared haplotypes were later than the enlarging of aridification (Fig 3). The predication was confirmed by the low molecular variance between groups (2.52%, Table 3). Therefore, the disjunctive distribution of *P. kansuensis* was unlikely the result of a range fragmentation, but shaped by long-distance dispersal crossing the wide arid land. Generally, long-distance dispersal is characterized by a movement from high genetic diversity region to low genetic diversity region [23,25]. The index of genetic diversity ( $H_T$ ) of the QTPG is significant higher than the TSG ( $H_T = 0.880$  vs.  $H_T = 0.753$ ) (Table 2). By this token, long-distance dispersal throughout arid land from the QTP, especially the northeast of the QTP, to the TSR could be the reason for the disjunctive distribution of *P. kansuensis*. In *P. longiflora*, the single haplotype that genetically connected the Altay Mts. with the NE of the QTP was also estimated to have diverged around 0.138 Mya. Both *P. longiflora* and *P. kansuensis* show lower level of genetic diversity in the Tianshan-Altay region than of the QTP. Given that the cradle of the genus *Pedicularis* is likely in the Hengduan-Himalayan Mts. at the SE of the QTP [100], the NW Chinese Tianshan and Altay Mts. were presumably colonized from the QTP earliest during the last interglacial of the late Pleistocene [87]. At that time the arid land barrier between the different mountain ranges as seen today must have been discontinuous to allow for seed flow. Evidence for this scenario is however lacking.

The species distribution model (SDM) results show an absence of *P. kansuensis* from the TSR during the LGM (Fig 5). This indicates that colonization must have occurred after the LGM, hence rather recently. This corroborates the genetic findings. Nevertheless, the reliability of the SDM is to be taken with caution as we failed to detect any range expansion or contraction in the QTP which would be an intuitive assumption (Table 3, Fig 3).

### Conclusion

Based on phylogeographical and species distribution modeling analyses, we propose that *P. kansuensis* has survived on the QTP throughout the LGM. The present day disjunct distribution in

the Qinghai-Tibetan Plateau and the Tianshan Region is likely the result of multiple bird or human assisted long-distance seed dispersal events crossing the arid land of Tarim Basin after the LGM, particularly from the northeastern fringes of the QTP to the Tianshan Mts.

## Supporting Information

**S1 Table.** The detailed voucher specimens information for used samples, including out-group, and the GenBank accession numbers of the used sequences. (DOCX)

## Acknowledgments

We thank Yuan-Xue Lu and Jun Lu for their kind help in collecting materials, Zhi-Hao Su, Hong-Xiang Zhang and Xiao-Jun Shi for their assistance in data analysis.

## Author Contributions

**Conceptualization:** ARL KYG.

**Data curation:** WJL ARL KYG.

**Formal analysis:** WJL PK ARL.

**Funding acquisition:** ARL KYG.

**Investigation:** WJL XLS.

**Methodology:** ARL KYG.

**Project administration:** KYG.

**Resources:** WJL XLS YYL.

**Supervision:** KYG.

**Writing – original draft:** WJL PK ARL.

**Writing – review & editing:** WJL PK ARL.

## References

1. Comes HP, Kadereit JW (1998) The effect of Quaternary climatic changes on plant distribution and evolution. *Trends in Plant Science* 3: 432–438.
2. Hewitt GM (2000) The genetic legacy of the Quaternary ice ages. *Nature* 405: 907–913. doi: [10.1038/35016000](https://doi.org/10.1038/35016000) PMID: [10879524](https://pubmed.ncbi.nlm.nih.gov/10879524/)
3. Hewitt GM (2004) Genetic consequences of climatic oscillations in the Quaternary. *Philosophical Transactions of the Royal Society of London Series B-Biological Sciences* 359: 183–195.
4. Qiu YX, Fu CX, Comes HP (2011) Plant molecular phylogeography in China and adjacent regions: tracing the genetic imprints of Quaternary climate and environmental change in the world's most diverse temperate flora. *Molecular Phylogenetics and Evolution* 59: 225–244. doi: [10.1016/j.ympev.2011.01.012](https://doi.org/10.1016/j.ympev.2011.01.012) PMID: [21292014](https://pubmed.ncbi.nlm.nih.gov/21292014/)
5. Raymo ME, Ruddiman WF (1992) Tectonic forcing of Late Cenozoic climate. *Nature* 359: 117–122.
6. Ruddiman WF, Kutzbach JE (1991) Plateau uplift and climatic-change. *Scientific American* 264: 66–75.
7. An ZS, Kutzbach JE, Prell WL, Porter SC (2001) Evolution of Asian monsoons and phased uplift of the Himalaya-Tibetan plateau since Late Miocene times. *Nature* 411: 62–66. doi: [10.1038/35075035](https://doi.org/10.1038/35075035) PMID: [11333976](https://pubmed.ncbi.nlm.nih.gov/11333976/)
8. Tang LY, Shen CM (1996) Late Cenozoic vegetational history and climatic characteristics of Qinghai-Xizang Plateau. *Acta Micropalaeontologica Sinica* 13: 321–338.

9. Shi YF, Li JJ, Li BY (1998) Uplift and environmental changes of Qinghai-Tibetan Plateau in the Late Cenozoic. Guangdong Science and Technology Press, Guangzhou. 1998.
10. Clark MK, House MA, Royden LH, Whipple KX, Burchfiel BC, et al. (2005) Late Cenozoic uplift of southeastern Tibet. *Geology* 33: 525–528.
11. Li GJ, Pettke T, Chen J (2011) Increasing Nd isotopic ratio of Asian dust indicates progressive uplift of the north Tibetan Plateau since the middle Miocene. *Geology* 39: 199–202.
12. Sun JM, Zhu RX, Bowler J (2004) Timing of the Tianshan Mountains uplift constrained by magnetotratigraphic analysis of molasse deposits. *Earth and Planetary Science Letters* 219: 239–253.
13. Sun J, Ding Z, Liu T (1998) Desert distributions during the glacial maximum and climatic optimum: example of China. *Episodes-News magazine of the International Union of Geological Sciences* 21: 28–31.
14. Xu ZQ, He BZ, Zhang CL, Zhang JX, Wang ZM, et al. (2013) Tectonic framework and crustal evolution of the Precambrian basement of the Tarim Block in NW China: new geochronological evidence from deep drilling samples. *Precambrian Research* 235: 150–162.
15. Kropf M, Comes HP, Kadereit JW (2006) Long-distance dispersal vs vicariance: the origin and genetic diversity of alpine plants in the Spanish Sierra Nevada. *New Phytologist* 172: 169–184. doi: [10.1111/j.1469-8137.2006.01795.x](https://doi.org/10.1111/j.1469-8137.2006.01795.x) PMID: [16945099](https://pubmed.ncbi.nlm.nih.gov/16945099/)
16. Villaverde T, Escudero M, Luceno M, Martin-Bravo S (2015) Long-distance dispersal during the middle-late Pleistocene explains the bipolar disjunction of *Carex maritima* (Cyperaceae). *Journal of Biogeography* 42: 1820–1831.
17. Gussarova G, Allen GA, Mikhaylova Y, McCormick LJ, Mirre V, Marr KL et al. (2015) Vicariance, long-distance dispersal, and regional extinction-recolonization dynamics explain the disjunct circumpolar distribution of the arctic-alpine plant *Silene acaulis*. *American Journal of Botany* 102: 1703–1720. doi: [10.3732/ajb.1500072](https://doi.org/10.3732/ajb.1500072) PMID: [26437887](https://pubmed.ncbi.nlm.nih.gov/26437887/)
18. Bendiksby M, Mazzoni S, Jorgensen MH, Halvorsen R, Holien H (2014) Combining genetic analyses of archived specimens with distribution modelling to explain the anomalous distribution of the rare lichen *Staurolemma omphalarioides*: long-distance dispersal or vicariance? *Journal of Biogeography* 41: 2020–2031.
19. Meng HH, Zhang ML (2013) Diversification of plant species in arid Northwest China: species-level phylogeographical history of *Lagochilus* Bunge ex Benth (Lamiaceae). *Molecular Phylogenetics and Evolution* 68: 398–409. doi: [10.1016/j.ympev.2013.04.012](https://doi.org/10.1016/j.ympev.2013.04.012) PMID: [23629053](https://pubmed.ncbi.nlm.nih.gov/23629053/)
20. Gao XY, Meng HH, Zhang ML (2014) Diversification and vicariance of desert plants: evidence inferred from chloroplast DNA sequence variation of *Lagochilus ilicifolius* (Lamiaceae). *Biochemical Systematics and Ecology* 55: 93–100.
21. Guo YP, Zhang R, Chen CY, Zhou DW, Liu JQ (2010) Allopatric divergence and regional range expansion of *Juniperus sabina* in China. *Journal of Systematics and Evolution* 48: 153–160.
22. Zhang HX, Zhang ML, Sanderson SC (2013) Retreating or standing: responses of forest species and steppe species to climate change in arid Eastern Central Asia. *PLoS One* 8: e61954. doi: [10.1371/journal.pone.0061954](https://doi.org/10.1371/journal.pone.0061954) PMID: [23596532](https://pubmed.ncbi.nlm.nih.gov/23596532/)
23. de Groot GA, Hofmeester TR, La Haye M, Jansman HAH, Perez-Haro M, Koelewijn HP (2016) Hidden dispersal in an urban world: genetic analysis reveals occasional long-distance dispersal and limited spatial substructure among Dutch pine martens. *Conservation Genetics* 17: 111–123.
24. Ram MS, Marne M, Gaur A, Kumara HN, Singh M, Kumar A, et al. (2015) Pre-Historic and recent vicariance events shape genetic structure and diversity in endangered Lion-Tailed Macaque in the Western Ghats: implications for conservation. *PLoS One* 10: e0142597. doi: [10.1371/journal.pone.0142597](https://doi.org/10.1371/journal.pone.0142597) PMID: [26561307](https://pubmed.ncbi.nlm.nih.gov/26561307/)
25. Friar EA, Ladoux T, Roalson EH, Robichaux RH (2000) Microsatellite analysis of a population crash and bottleneck in the Mauna Kea silversword, *Argyroxiphium sandwicense* ssp. *sandwicense* (Asteraceae), and its implications for reintroduction. *Molecular Ecology* 9: 2027–2034. PMID: [11123615](https://pubmed.ncbi.nlm.nih.gov/11123615/)
26. Nybom H (2004) Comparison of different nuclear DNA markers for estimating intraspecific genetic diversity in plants. *Molecular Ecology* 13: 1143–1155. doi: [10.1111/j.1365-294X.2004.02141.x](https://doi.org/10.1111/j.1365-294X.2004.02141.x) PMID: [15078452](https://pubmed.ncbi.nlm.nih.gov/15078452/)
27. Nybom N, Bartish I (2000) Effects of life history traits and sampling strategies on genetic diversity estimates obtained with RAPD markers in plants. *Perspectives in Plant Ecology Evolution and Systematics* 3: 93–114.
28. Wen J, Zhang JQ, Nie ZL, Zhong Y, Sun H (2014) Evolutionary diversifications of plants on the Qinghai-Tibetan Plateau. *Frontiers in Genetics* 5. doi: [10.3389/fgene.2014.00004](https://doi.org/10.3389/fgene.2014.00004) PMID: [24575120](https://pubmed.ncbi.nlm.nih.gov/24575120/)
29. Liu JQ, Sun YS, Ge XJ, Gao LM, Qiu YX (2012) Phylogeographic studies of plants in China: advances in the past and directions in the future. *Journal of Systematics and Evolution* 50: 267–275.



30. Shi XJ, Zhang ML (2015) Phylogeographical structure inferred from cpDNA sequence variation of *Zygophyllum xanthoxylon* across north-west China. *Journal of Plant Research* 128: 269–282. doi: [10.1007/s10265-014-0699-y](https://doi.org/10.1007/s10265-014-0699-y) PMID: [25626403](https://pubmed.ncbi.nlm.nih.gov/25626403/)
31. Jiang XL, Zhang ML, Zhang HX, Sanderson SC (2014) Phylogeographic patterns of the *Aconitum nemorum* species group (Ranunculaceae) shaped by geological and climatic events in the Tianshan Mountains and their surroundings. *Plant Systematics and Evolution* 300: 51–61.
32. Zhang JQ, Meng SY, Rao GY (2014) Phylogeography of *Rhodiola kirilowii* (Crassulaceae): a story of Miocene divergence and Quaternary expansion. *PLoS One* 9: e112923. doi: [10.1371/journal.pone.0112923](https://doi.org/10.1371/journal.pone.0112923) PMID: [25389750](https://pubmed.ncbi.nlm.nih.gov/25389750/)
33. Zhang HX, Zhang ML (2012) Identifying a contact zone between two phylogeographic lineages of *Clematis sibirica* (Ranunculaceae) in the Tianshan and Altai Mountains. *Journal of Systematics and Evolution* 50: 295–304.
34. Zhang HX, Zhang ML (2012) Genetic structure of the *Delphinium naviculare* species group tracks Pleistocene climatic oscillations in the Tianshan Mountains, arid Central Asia. *Palaeogeography, Palaeoclimatology, Palaeoecology* 353–355: 93–103.
35. Yang FS, Li YF, Ding X, Wang XQ (2008) Extensive population expansion of *Pedicularis longiflora* (Orobanchaceae) on the Qinghai-Tibetan Plateau and its correlation with the Quaternary climate change. *Molecular Ecology* 17: 5135–5145. doi: [10.1111/j.1365-294X.2008.03976.x](https://doi.org/10.1111/j.1365-294X.2008.03976.x) PMID: [19017264](https://pubmed.ncbi.nlm.nih.gov/19017264/)
36. Wang L, Wu ZQ, Bystriakova N, Ansell SW, Xiang QP, Heinrichs J, et al. (2011) Phylogeography of the Sino-Himalayan fern *Lepisorus clathratus* on “the roof of the world”. *PLoS One* 6: e25896. doi: [10.1371/journal.pone.0025896](https://doi.org/10.1371/journal.pone.0025896) PMID: [21984953](https://pubmed.ncbi.nlm.nih.gov/21984953/)
37. Chen JM, Du ZY, Sun SS, Gituru RW, Wang QF (2013) Chloroplast DNA phylogeography reveals repeated range expansion in a widespread aquatic herb *Hippuris vulgaris* in the Qinghai-Tibetan Plateau and adjacent areas. *PLoS One* 8: e60948. doi: [10.1371/journal.pone.0060948](https://doi.org/10.1371/journal.pone.0060948) PMID: [23565290](https://pubmed.ncbi.nlm.nih.gov/23565290/)
38. Li KH, Hu YK, Adeli M, Lu CF, Yu JM, Liu YY (2006) Impact of temperature on seed germination of *Pedicularis verticillata* (Scrophulariaceae). *Acta Botanica Yunnanica* 28: 421–424.
39. Wang WL, Wang JY, Chen AL, Hu YK, Liu YY (2010) Study of *Pedicularis verticillata*'s chemical control. *Xinjiang Agricultural Sciences* 47: 1242–1247.
40. Liu YY, Hu YK, Wang X, Gong YM, Li KH (2011) Studies on characteristics of soil seed bank of *Pedicularis verticillata* community. *Journal of Natural Resources* 26: 48–57.
41. Sui XL, Li AR, Guan KY (2013) Impacts of climatic changes as well as seed germination characteristics on the population expansion of *Pedicularis verticillata*. *Ecology and Environmental Sciences* 22: 1099–1104.
42. Sui XL, Kuss P, Li WJ, Yang MQ, Guan KY, et al. (2016) Identity and distribution of weedy *Pedicularis kansuensis* Maxim. (Orobanchaceae) in Xinjiang Tianshan Mountains: morphological, anatomical and molecular evidence. *Journal of Arid Land* 8: 453–461.
43. Yang HB, Holmgren N, Mill R. *Pedicularis* L. In: Wu ZY, Raven PH, Hong DY (eds), *Flora of China*. Science Press, Beijing, and Missouri Botanical Garden Press, St. Louis. 1998; 18: pp 97–209.
44. Sui XL, Huang W, Li YJ, Guan KY, Li AR (2015) Host shoot clipping depresses the growth of weedy hemiparasitic *Pedicularis kansuensis*. *Journal of Plant Research* 128: 563–572. doi: [10.1007/s10265-015-0727-6](https://doi.org/10.1007/s10265-015-0727-6) PMID: [25956077](https://pubmed.ncbi.nlm.nih.gov/25956077/)
45. Taberlet P, Gielly L, Pautou G, Bouvet J (1991) Universal primers for amplification of three noncoding regions of chloroplast DNA. *Plant Molecular Biology* 17: 1105–1109. PMID: [1932684](https://pubmed.ncbi.nlm.nih.gov/1932684/)
46. Shaw J, Lickey EB, Schilling EE, Small RL (2007) Comparison of whole chloroplast genome sequences to choose noncoding regions for phylogenetic studies in angiosperms: the tortoise and the hare III. *American Journal of Botany* 94: 275–288. doi: [10.3732/ajb.94.3.275](https://doi.org/10.3732/ajb.94.3.275) PMID: [21636401](https://pubmed.ncbi.nlm.nih.gov/21636401/)
47. Thompson JD, Higgins DG, Gibson TJ (1994) CLUSTAL W: improving the sensitivity of progressive multiple sequence alignment through sequence weighting, position-specific gap penalties and weight matrix choice. *Nucleic Acids Research* 22: 4673–4680. PMID: [7984417](https://pubmed.ncbi.nlm.nih.gov/7984417/)
48. Librado P, Rozas J (2009) DnaSP v5: a software for comprehensive analysis of DNA polymorphism data. *Bioinformatics* 25: 1451–1452. doi: [10.1093/bioinformatics/btp187](https://doi.org/10.1093/bioinformatics/btp187) PMID: [19346325](https://pubmed.ncbi.nlm.nih.gov/19346325/)
49. Excoffier L, Lischer HE (2010) ARLEQUIN suite ver 3.5: a new series of programs to perform population genetics analyses under Linux and Windows. *Molecular Ecology Resources* 10: 564–567. doi: [10.1111/j.1755-0998.2010.02847.x](https://doi.org/10.1111/j.1755-0998.2010.02847.x) PMID: [21565059](https://pubmed.ncbi.nlm.nih.gov/21565059/)
50. Leberg PL (2002) Estimating allelic richness: effects of sample size and bottlenecks. *Molecular Ecology* 11: 2445–2449. PMID: [12406254](https://pubmed.ncbi.nlm.nih.gov/12406254/)
51. R Core Team (2016) R: a language and environment for statistical computing. R Foundation for Statistical Computing. Vienna, Austria.

52. Dupanloup I, Schneider S, Excoffier L (2002) A simulated annealing approach to define the genetic structure of populations. *Molecular Ecology* 11: 2571–2581. PMID: [12453240](#)
53. Manni F, Guerard E, Heyer E (2004) Geographic patterns of (genetic, morphologic, linguistic) variation: how barriers can be detected by using Monmonier's algorithm. *Human Biology* 76: 173–190. PMID: [15359530](#)
54. Monmonier MS (1973) Maximum-Difference Barriers: an alternative numerical regionalization method. *Geographical Analysis* 5: 245–261.
55. Wright S (1943) Isolation by distance. *Genetics* 28:114–38. PMID: [17247074](#)
56. Slatkin M (1987) Gene flow and the geographic structure of natural populations. *Science* 236:787–92. PMID: [3576198](#)
57. Miller MP (2005) Alleles In Space (AIS): Computer software for the joint analysis of interindividual spatial and genetic information. *Journal of Heredity* 96: 722–724. doi: [10.1093/jhered/esi119](#) PMID: [16251514](#)
58. Excoffier L, Smouse PE, Quattro JM (1992) Analysis of molecular variance inferred from metric distances among DNA haplotypes: application to human mitochondrial-DNA restriction data. *Genetics* 131: 479–491. PMID: [1644282](#)
59. Pons O, Petit R (1996) Measuring and testing genetic differentiation with ordered versus unordered alleles. *Genetics* 144: 1237–1245. PMID: [8913764](#)
60. Tamura K, Stecher G, Peterson D, Filipowski A, Kumar S (2013) MEGA6: molecular evolutionary genetics analysis version 6.0. *Molecular Biology and Evolution* 30: 2725–2729. doi: [10.1093/molbev/mst197](#) PMID: [24132122](#)
61. Bandelt HJ, Forster P, Röhl A (1999) Median-joining networks for inferring intraspecific phylogenies. *Molecular Biology and Evolution* 16: 37–48. PMID: [10331250](#)
62. Drummond AJ, Suchard MA, Xie D, Rambaut A (2012) Bayesian phylogenetics with BEAUti and the BEAST 1.7 *Molecular Biology and Evolution* 29: 1969–1973. doi: [10.1093/molbev/mss075](#) PMID: [22367748](#)
63. Posada D, Crandall KA (1998) Modeltest: testing the model of DNA substitution. *Bioinformatics* 14: 817–818. PMID: [9918953](#)
64. Richardson JE, Pennington RT, Pennington TD, Hollingsworth PM (2001) Rapid diversification of a species-rich genus of neotropical rain forest trees. *Science* 293: 2242–2245. doi: [10.1126/science.1061421](#) PMID: [11567135](#)
65. Rambaut A, Drummond A (2009) TRACER v1.5.0. Available online: <http://beast.bio.ed.ac.uk/> (accessed on 10 Aug 2011).
66. Tajima F (1989) Statistical method for testing the neutral mutation hypothesis by DNA polymorphism. *Genetics* 123: 585–595. PMID: [2513255](#)
67. Fu YX, Li WH (1993) Statistical tests of neutrality of mutations. *Genetics* 133: 693–709. PMID: [8454210](#)
68. Harpending H (1994) Signature of ancient population growth in a low-resolution mitochondrial DNA mismatch distribution. *Human Biology* 591–600. PMID: [8088750](#)
69. Phillips SJ, Anderson RP, Schapire RE (2006) Maximum entropy modeling of species geographic distributions. *Ecological Modelling* 190: 231–259.
70. Hijmans RJ, Cameron SE, Parra JL, Jones PG, Jarvis A (2005) Very high resolution interpolated climate surfaces for global land areas. *International Journal of Climatology* 25: 1965–1978.
71. Collins WD, Bitz CM, Blackmon ML, Bonan GB, Bretherton CS, Chang P, et al. (2006) The community climate system model version 3 (CCSM3). *Journal of Climate* 19: 2122–2143.
72. Tkach N, Ree RH, Kuss P, Roeser M, Hoffmann MH (2014) High mountain origin, phylogenetics, evolution, and niche conservatism of arctic lineages in the hemiparasitic genus *Pedicularis* (Orobanchaceae). *Molecular Phylogenetics and Evolution* 76: 75–92. doi: [10.1016/j.ympev.2014.03.004](#) PMID: [24631857](#)
73. Kuss P, Ree RH (2015) Reproductive biology of *Pedicularis* (Orobanchaceae) in Nepal. In: Miehe G & Pendry CA (eds.). *Nepal. An introduction to the natural history, ecology and human environment of the Himalayas*. Edinburgh: Royal Botanic Garden Edinburgh.
74. Wang LY, Abbott RJ, Zheng W, Chen P, Wang YJ, Liu JQ (2009) History and evolution of alpine plants endemic to the Qinghai-Tibetan Plateau: *Aconitum gymnanthum* (Ranunculaceae). *Molecular Ecology* 18: 709–721. doi: [10.1111/j.1365-294X.2008.04055.x](#) PMID: [19175501](#)
75. Zhang XM, He XJ (2013) Phylogeography of *Angelica nitida* (Apiaceae) endemic to the Qinghai-Tibet Plateau based on chloroplast DNA sequences. *Journal of Systematics and Evolution* 51: 564–577.

76. Xu TT, Abbott RJ, Milne RI, Mao KS, Du FK, Wu G, et al. (2010) Phylogeography and allopatric divergence of cypress species (*Cupressus* L.) in the Qinghai-Tibetan Plateau and adjacent regions. *BMC Evolutionary Biology* 10:194. doi: [10.1186/1471-2148-10-194](https://doi.org/10.1186/1471-2148-10-194) PMID: [20569425](https://pubmed.ncbi.nlm.nih.gov/20569425/)
77. Wang JF, Gong X, Chiang YC, Kuroda C (2013) Phylogenetic patterns and disjunct distribution in *Ligularia hodgsonii* Hook. (Asteraceae). *Journal of Biogeography* 40: 1741–1754.
78. Reboud X, Zeyl C (1994) Organelle inheritance in plants. *Heredity* 72: 132–140.
79. Ennos R (1994) Estimating the relative rates of pollen and seed migration among plant populations. *Heredity* 72: 250–259.
80. Liu ML, Yu WB, Li DZ, Mill RR, Wang H (2013) Seed morphological diversity of *Pedicularis* (Orobanchaceae) and its taxonomic significance. *Plant Systematics and Evolution* 299: 1645–1657.
81. Prain D (1890) The species of *Pedicularis* of the Indian Empire and its frontiers. *Annals of the Royal Botanic Garden* 3:1–196.
82. Liu YY, Hu YK, Yu JM, Wang X, Li KH (2011) *Pedicularis verticillata* community characteristics along water gradient on alpine grassland. *Bulletin of Soil and Water Conservation* 31: 52–56, 65.
83. Hu RJ (2004) Physical geography of the Tianshan Mountains in China. Beijing: China Environmental Science Press.
84. Pellerin M, Picard M, Said S, Baubet E, Baltzinger C (2016) Complementary endozoochorous long-distance seed dispersal by three native herbivorous ungulates in Europe. *Basic and Applied Ecology* 17: 321–332.
85. Cancio I, Gonzalez-Robles A, Bastida JM, Manzaneda AJ, Salido T, et al. (2016) Habitat loss exacerbates regional extinction risk of the keystone semiarid shrub *Ziziphus lotus* through collapsing the seed dispersal service by foxes (*Vulpes vulpes*). *Biodiversity and Conservation* 25: 693–709.
86. Li N, Li XH, An SQ, Lu CH (2016) Impact of multiple bird partners on the seed dispersal effectiveness of China's relic trees. *Scientific Reports* 6: 17489–17489. doi: [10.1038/srep17489](https://doi.org/10.1038/srep17489) PMID: [26725517](https://pubmed.ncbi.nlm.nih.gov/26725517/)
87. Zheng B, Xu Q, Shen Y (2002) The relationship between climate change and Quaternary glacial cycles on the Qinghai-Tibetan Plateau: review and speculation. *Quaternary International* 97: 93–101.
88. Zhou SZ, Wang XL, Wang J, Xu LB (2006) A preliminary study on timing of the oldest Pleistocene glaciation in Qinghai-Tibetan Plateau. *Quaternary International* 154: 44–51.
89. Abbott RJ, Smith LC, Milne RI, Crawford RM, Wolff K, Balfour J (2000) Molecular analysis of plant migration and refugia in the Arctic. *Science* 289: 1343–1346. PMID: [10958779](https://pubmed.ncbi.nlm.nih.gov/10958779/)
90. Chen SY, Wu GL, Zhang DJ, Gao QB, Duan YZ, Zhang FQ, et al. (2008) Potential refugium on the Qinghai-Tibet Plateau revealed by the chloroplast DNA phylogeography of the alpine species *Metagentiana striata* (Gentianaceae). *Botanical Journal of the Linnean Society* 157: 125–140.
91. Zou JB, Peng XL, Li L, Liu JQ, Miehle G, Opgenoorth L (2012) Molecular phylogeography and evolutionary history of *Picea likiangensis* in the Qinghai-Tibetan Plateau inferred from mitochondrial and chloroplast DNA sequence variation. *Journal of Systematics and Evolution* 50: 341–350.
92. Yang FS, Qin AL, Li YF, Wang XQ (2012) Great genetic differentiation among populations of *Mecynopsis integrifolia* and its implication for plant speciation in the Qinghai-Tibetan Plateau. *PLoS One* 7: e37196. doi: [10.1371/journal.pone.0037196](https://doi.org/10.1371/journal.pone.0037196) PMID: [22590654](https://pubmed.ncbi.nlm.nih.gov/22590654/)
93. Gao QB, Zhang DJ, Duan YZ, Zhang FQ, Li YH, Fu PC, et al. (2012) Intraspecific divergences of *Rhodiola alsia* (Crassulaceae) based on plastid DNA and internal transcribed spacer fragments. *Botanical Journal of the Linnean Society* 168: 204–215.
94. Li Y, Stocks M, Hemmälä S, Källman T, Zhu HT, Zhou YF, et al. (2010) Demographic histories of four spruce (*Picea*) species of the Qinghai-Tibetan Plateau and neighboring areas inferred from multiple nuclear loci. *Molecular Biology and Evolution* 27: 1001–1014. doi: [10.1093/molbev/msp301](https://doi.org/10.1093/molbev/msp301) PMID: [20031927](https://pubmed.ncbi.nlm.nih.gov/20031927/)
95. Meng L, Yang R, Abbott RJ, Miehle G, Hu T, Liu J (2007) Mitochondrial and chloroplast phylogeography of *Picea crassifolia* Kom. (Pinaceae) in the Qinghai-Tibetan Plateau and adjacent highlands. *Molecular Ecology* 16: 4128–4137. doi: [10.1111/j.1365-294X.2007.03459.x](https://doi.org/10.1111/j.1365-294X.2007.03459.x) PMID: [17894761](https://pubmed.ncbi.nlm.nih.gov/17894761/)
96. Wang ZJ, Guan KY (2011) Genetic structure and phylogeography of a relict tree fern, *Sphaeropteris brunoniana* (Cyatheaceae) from China and Laos inferred from cpDNA sequence variations: Implications for conservation. *Journal of Systematics and Evolution* 49: 72–79.
97. Gao LM, Moller M, Zhang XM, Hollingsworth ML, Liu J, Mill RR, et al. (2007) High variation and strong phylogeographic pattern among cpDNA haplotypes in *Taxus wallichiana* (Taxaceae) in China and North Vietnam. *Molecular Ecology* 16: 4684–4698. doi: [10.1111/j.1365-294X.2007.03537.x](https://doi.org/10.1111/j.1365-294X.2007.03537.x) PMID: [17908214](https://pubmed.ncbi.nlm.nih.gov/17908214/)

98. Stewart JR, Lister AM, Barnes I, Dalen L (2010) Refugia revisited: individualistic responses of species in space and time. *Proceedings of the Royal Society B-Biological Sciences* 277: 661–671.
99. Williams MJ, Dunkerley DL, De Dekker P, Kershaw AP, Stokes T (1993) Quaternary environments. London: Edward Arnold.
100. Ree RH (2005) Phylogeny and the evolution of floral diversity in *Pedicularis* (Orobanchaceae). *International Journal of Plant Sciences* 166: 595–613.